GeoStudio Example File

Cubzac-les-Ponts Experimental Embankments on Soft Clay

To see the latest GeoStudio learning content, visit Seequent Learning Centre and search the catalogue for “GeoStudio”.

Introduction

In the 1970's, a series of test embankments were constructed on soft clay at Cubzac-les-Ponts in France. These full-scale field tests were well-instrumented and are well-documented, and consequently provide an excellent case history. Two of the embankments are the subject of this example. Embankment A was built rapidly to failure to find the limiting height. Embankment B was later constructed to a lower height, to study the long term, time-dependent consolidation of the soft foundation clay.

The purpose here is to demonstrate that GeoStudio has the features and capability to numerically simulate the deformations and stability of such embankments using a fully coupled effective stress/pore-water pressure type of analysis. There are many publications describing the tests, analyses and experiments carried out at Cubzac-les-Ponts. The data used to develop the analyses here was extracted from the books written by Wood (1990) and Leroueil et al. (1990). The rest of this article refers to these authors as the Researchers.

Numerical Simulation

At the Cubzac-les-Ponts site, the upper two metres of the clay deposit is desiccated and over-consolidated due to the seasonal variations in the water table. For analysis purposes, the water table is taken to be at a depth of 1 m. Below the upper desiccated crust there is a 7-m thick stratum of slightly over-consolidated soft clay. It is the performance of this soft clay that was at the heart of the field research.

Under the clay stratum there is coarse sand and gravel with a relatively high hydraulic conductivity. The static pressure head in the gravel is about 8 m, making the pore-water pressure distribution more or less hydrostatic within the clay. For modelling purposes, it is assumed that the pore-water pressure in the underlying granular material will not change due to the embankment loading.

The original researchers divided the soft clay into many different layers with slightly different properties. This refinement is not considered here. Both the upper crust and the underlying clay are simplified to be homogeneous isotropic soil units. This simplification does not seem to have a significant effect on the results, since the computed values are in reasonable agreement with values computed by others and with the field measurements.

The stress-strain response of the soft clay is assumed to be represented by the modified Cam clay constitutive model. The model is formulated on the classical elastic-plastic framework and exhibits hardening or softening behaviour depending on the overconsolidation state. Moderately overconsolidated to normally compressed soils therefore exhibit excess pore-water pressures due to a tendency for both elastic and plastic volumetric straining, which is an important aspect of soft clay behavior.

The soil properties used to represent the stress-strain behavior and strength of the soft clay are shown in Table 1. The stiffness of the soil is controlled by the slopes of the isotropic normal compression line (Lambda) and the unloading-reloading line (Kappa).

Table 1. Soil properties for the soft clay.

Parameter	Value
Constitutive model	Modified Cam-Clay
Over-consolidation Ratio:	1.4
Poisson's Ratio (ν):	0.4
Lambda (λ):	0.5
Kappa (κ):	0.05
Initial Void Ratio:	2.25
Mu (M) ($\phi' = 30^{\circ}$):	1.2
Unit Weight (γ; kN / m^3):	15.0
K_{sat} m/day	1 x 10^{-4}

In a SIGMA/W consolidation analysis, it is necessary to define the hydraulic properties for each material. The clay remains saturated throughout the duration of the analysis and is therefore defined using a saturated-only material model. The properties used for the desiccated crust are listed in Table 2. The effective strength parameters are listed, since they are used in the stability analysis.

Table 2. Soil properties for the desiccated crust.

Parameter	Value
Constitutive model	Linear-elastic
Young's Modulus *E* (kPa):	3000
Poisson's Ratio (ν):	0.4
Unit Weight (γ; kN / m^3):	16.5
Effective Friction Angle:	30°
Cohesion (kPa)	0
K_{sat} m/day	8 x 10^{-4}

The water table is at mid-depth of the upper crust making the pore-water pressure negative above the water table. To handle this correctly in a saturated-unsaturated consolidation analysis, it is necessary to define a VWC function and a hydraulic conductivity function. Figure 1 shows the VWC function of the desiccated crust that was estimated from the built-in sample functions. The function was generated using a saturated volumetric water content of 0.3 with all other parameters at the default values.

The air entry value (AEV) for this VWC function is around 10 kPa suction. This implies that the soil above the water table is more or less saturated, but the pore-water pressure is negative. This is referred to as a tension-saturated zone. It means that the pore-water pressure will become positive quickly as the embankment load is applied.

Figure 2 shows the hydraulic conductivity function used for the desiccated crust. It was estimated from the volumetric water content function using the van Genuchten technique. The function was generated using a saturated hydraulic conductivity of 8.0 x 10^{-4} m/day (approximately 1 x 10^{-8} m/sec) and a residual volumetric water content of 0.04. All other parameters were left at the default values.

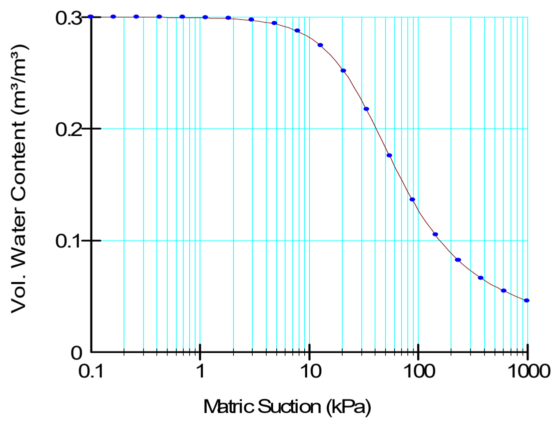

Figure 1. Volumetric water content function for the crust.

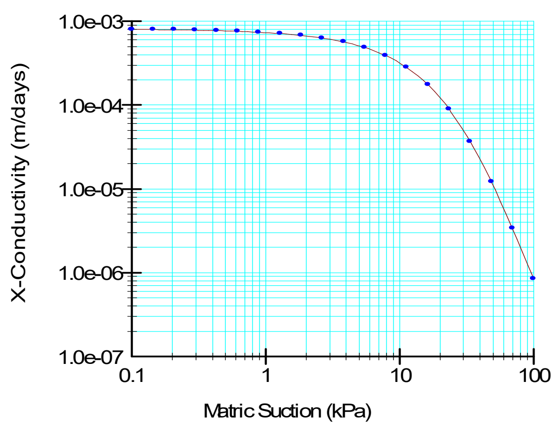

Figure 2. Hydraulic conductivity function for the desiccated crust.

The embankment fill is modelled using a isotropic linear elastic model (Table 3).The material used for the embankment construction is coarse sand and gravel. As such, the saturated-only material was used to define the hydraulic properties, with a large saturated conductivity of 1 m/day to promote rapid drainage. Finally, the option for ‘No change in water pressure due to volumetric strain’ is toggled on to ensure that self-weight generated pore-water pressure do not develop.

Table 3. Soil properties for the embankment fill.

Parameter	Value
Model:	Linear-Elastic
Young's Modulus E (kPa):	3000
Poisson's Ratio (ν):	0.4
Unit Weight (γ; kN / m³):	21.0
Effective Friction Angle:	35°
Cohesion (kPa)	0 kPa

Embankment A

As noted in the introduction, Embankment A was constructed rapidly to determine the height or conditions at which failure would occur. The cross-section used to model this part of the field experiment is shown in Figure 3. First, a 1.5 m lift was placed over a wide area. Next, three 1 m lifts were placed to one side to ensure that the failure would be to the right.

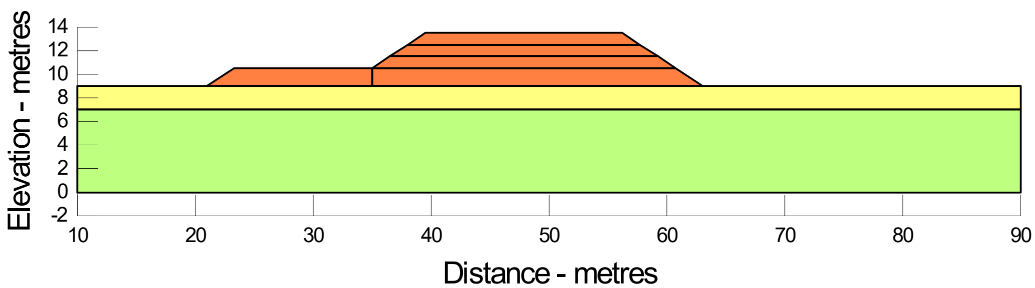

Figure 3. Embankment A used to determine failure conditions.

The fill was placed over a period of eight days. On Day 1, the fill reached 1.5 m. Additional 1 m lifts were placed on Day 5, Day 7 and Day 8. This sequence is detailed in the SIGMA/W time stepping specification.

The analysis tree is given in Figure 4. The first analysis establishes the *in situ* stress condition before the fill placement starts. Lift 1 is placed on Day 1, but the analysis covers 4 days. Lift 2 has a time-duration of 2 days. Lifts 3 and 4 each have a time-duration of 1 day. The fill placement took place over 8 days when the failure started. The last analysis is a slope stability analysis used to compute the factor of safety when the failure started.

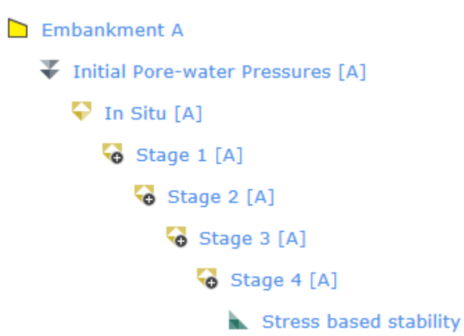

Figure 4. Embankment A analysis tree.

At the start of the analysis, it is not known how much the water table will rise due to the loading. The possibility of the water table coming up to contact the base of the fill can be covered with the specification of a potential seepage face review boundary. The effect of this is that if the computed total head is greater than the elevation, the boundary condition is converted to a Head-type, with the action equal to the y-coordinate, which represents zero pore-water pressure. A total head of 9 m was applied as a boundary condition to the base of the domain.

Embankment B

Embankment B (Figure 5) was constructed to a height of 2.4 m over a period of six days. For this analysis, the fill placement is simulated with six even lifts, one lift per day. Settlements, pore-water pressures and lateral deformations were then monitored over the next five years.

The material properties for Embankment B are the same as for Embankment A. The analysis tree for Embankment B is shown in Figure 6.

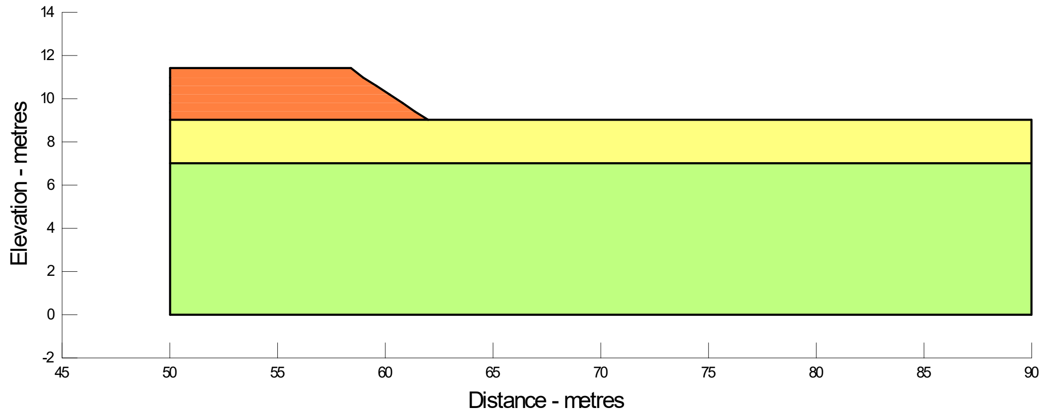

Figure 5. Embankment B configuration.

Figure 6. Analysis tree for Embankment B.

Results and Discussion

Embankment A

Figure 7 presents the effective stress profiles for the Gravity Activation *In Situ* analysis. Both materials are defined with a Poisson's ratio of 0.4, making K_0 equal to 0.667. At the base of the column, the y-effective and x-effective stress is about 60 kPa and 40 kPa, respectively. The effective stress profiles in the upper crust is slightly curved because the influence of negative pore-water pressure is weighted by the effective degree of saturation (see SIGMA/W reference book).

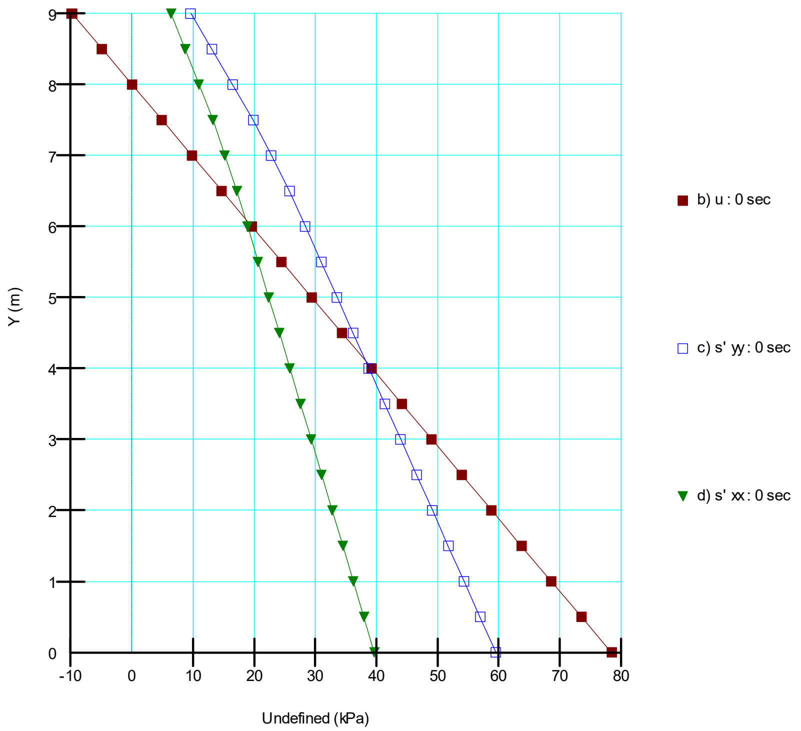

Figure 7. Effective stress profiles for the *in situ* stress analysis.

The water table rises slightly when the first lift is placed (Figure 9). By the end of the fill placement, the water table (zero pore-water pressure line) has reached the base of the fill (Figure 10). The fill material drains rapidly due to the high hydraulic conductivity.

Figure 9. Position of the water table on Day 1 after first lift.

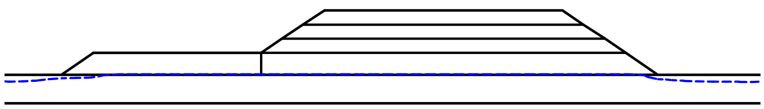

Figure 10. Position of water table after last lift.

Figure 11 demonstrates how the pore-water pressure increases with time at a point under the centre of the fill at the clay-fill contact level. Once the positive pore-water pressure reaches the contact level where the boundary condition is specified as potential seepage face, the pore-water pressure remains at zero (Day 6). This behavior is consistent with what one would intuitively expect, and demonstrates how SIGMA/W can correctly model saturated-unsaturated consolidation.

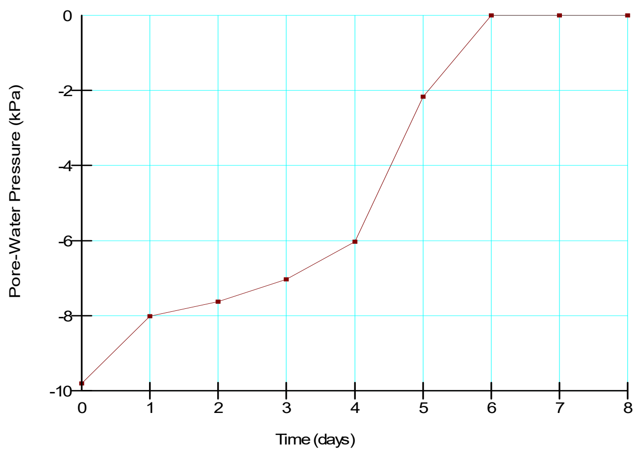

Figure 11. Pore-water pressure rise in crust with time during fill placement.

Figure 12 shows the settlement profiles at the four loading stages. The numbers beside the series symbols are days from start of construction. The maximum computed settlement is approximately 0.16 m (16 cm). The maximum measured settlement in the field was slightly greater than 20 cm. Of some interest is the unsymmetrical shape in the maximum settlement along the surface profile. The maximum tends to the right side, which reflects the movement in the direction of the failure. The simulated total settlement could easily be improved by better accommodating the spatial variability of the material parameters; however, the important point is that the computed and measured patterns of behavior are very similar. The agreement between measured and computed settlements is actually rather remarkable, in light of the complex spatial variations of material properties. Furthermore, the end of construction settlement reading was recorded when the foundation materials were in a failed state and therefore possibly accelerating.

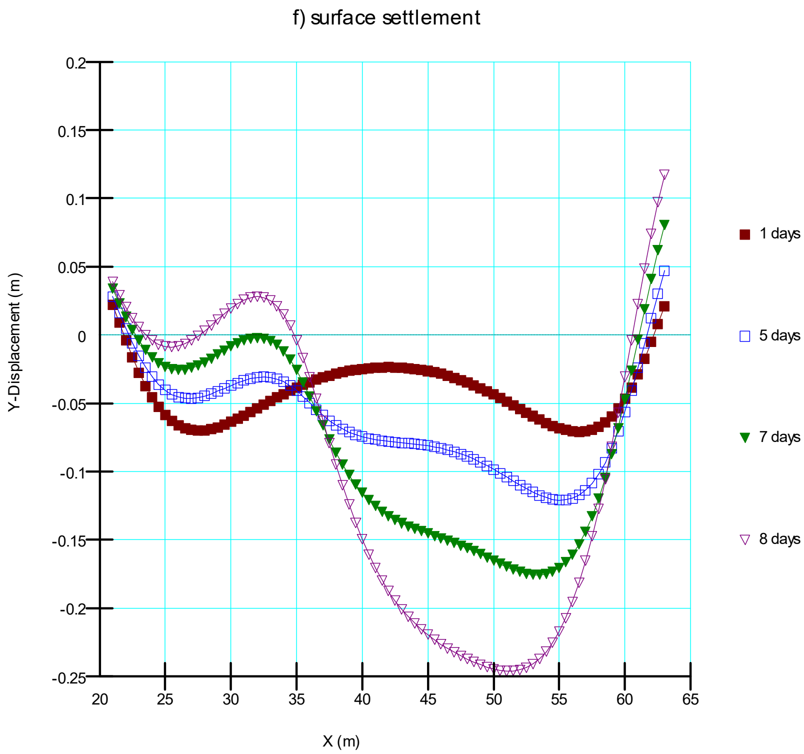

Figure 12. Settlement profiles under the embankment at the four loading stages.

Figure 13 shows the pore-water pressures in the foundation under the centre of the embankment. The maximum pore-water pressure is about 150 kPa, which is excess of the initial pore-water pressure by about 80 kPa upon completion of the fill placement, which is nearly identical to the values generated by finite element analyses of other researchers (generally between 80 and 100 kPa). The predictions at other stages (e.g. fill height of 3.5 m) are also in agreement with the work of other researchers.

.

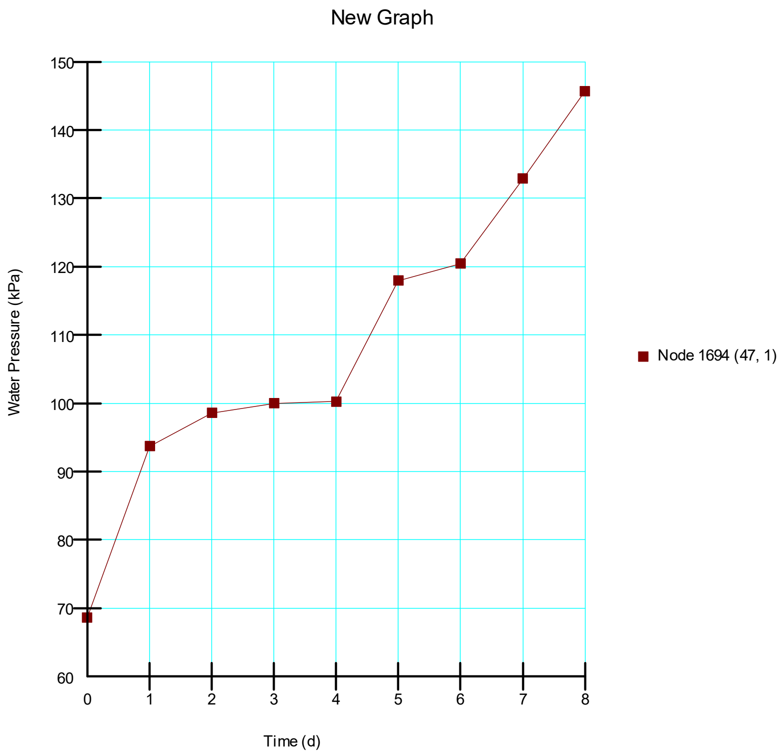

Figure 13. Excess pore-water pressure under the centre of the embankment.

After reaching a fill height of 4.5 m, the embankment failed. By definition, the factor of safety fell to 1.0. When the SIGMA/W computed stresses and pore-water pressures are used in a SLOPE/W stability analysis, the minimum factor of safety is approaching around 1.0 (Figure 14). This close agreement between the computed stability and the actual failure is notable.

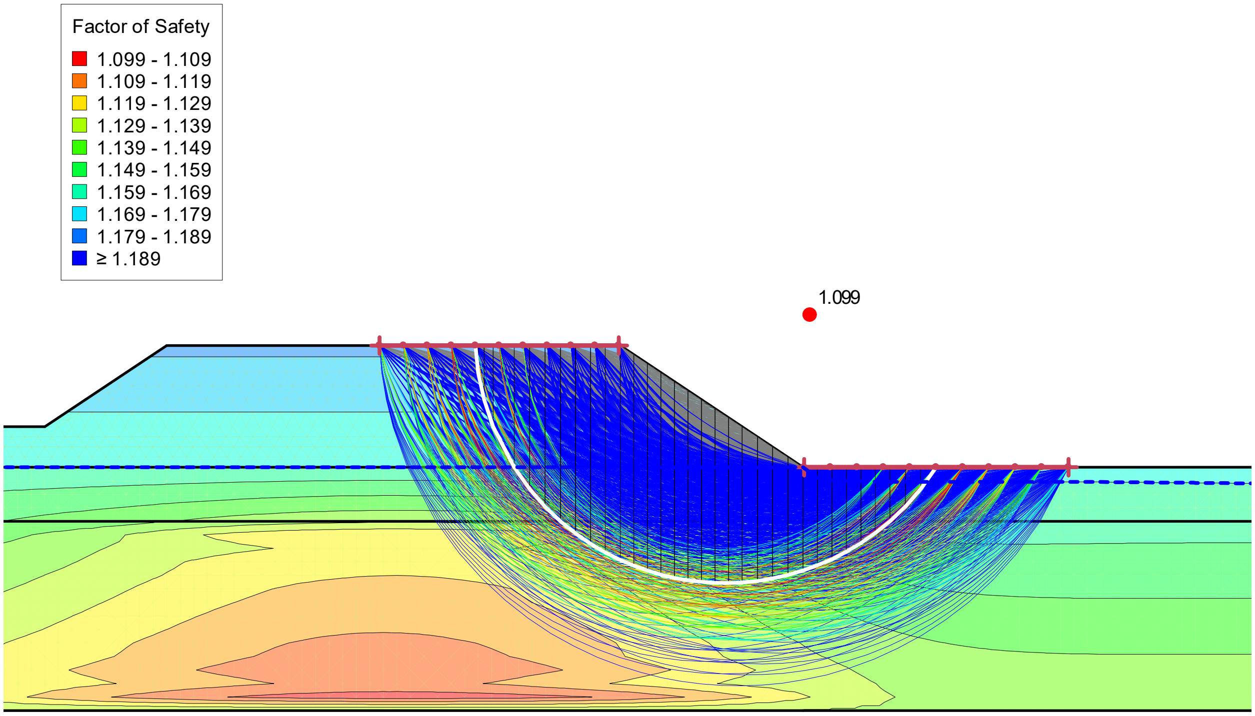

Figure 14. Computed stability safety factor at the time of failure.

Embankment B

The build-up of pore-water pressures due to the six days of embankment construction is shown in Figure 15 for Embankment B. The patterns of the field measured excess pore-water pressure profiles were considerably more variable (not as uniform) than those shown in Figure 15. The peak measured excess pore-water pressures, however, were in the range of 40 to 50 kPa, the same as the computed values at the end of the fill placement.

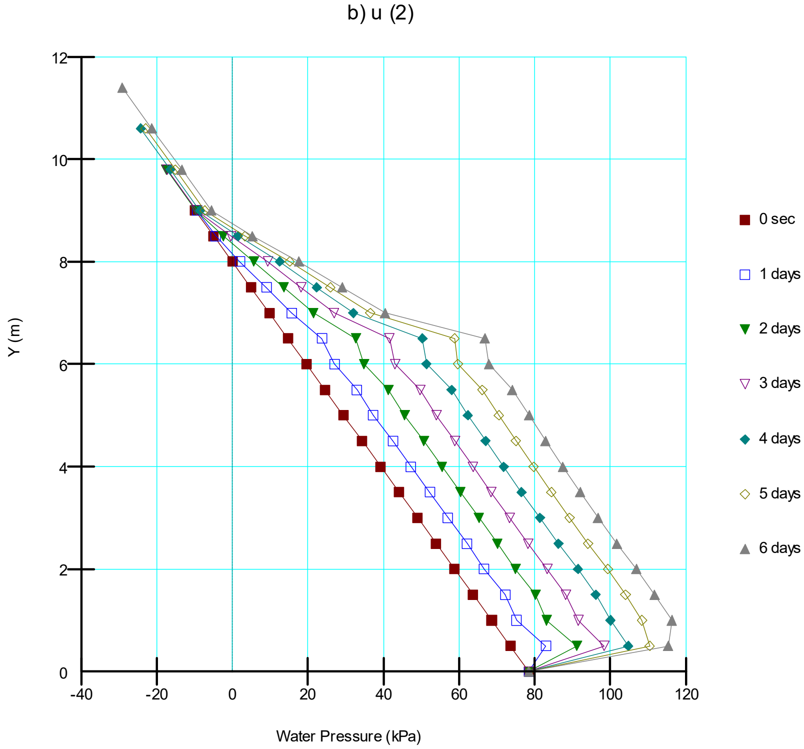

Figure 15. Buildup of excess pore-water pressures during fill placement.

During the long-term monitoring, the excess pore-water pressure dissipated (Figure 16). After 2006 days (5.5 years), the pore-water pressure has diminished to about 15 kPa in excess of the initial condition. This dissipation is somewhat greater than what happened in the field. The maximum measured values at the end of the same time period, however, were around 25 kPa above the initial value. The simulation could perhaps be improved by incorporating more of the actual spatial variations in the material properties. While the actual measured and computed values vary somewhat, the profile patterns and trends are remarkably similar. In this sense, the numerical model represents the field performance very well.

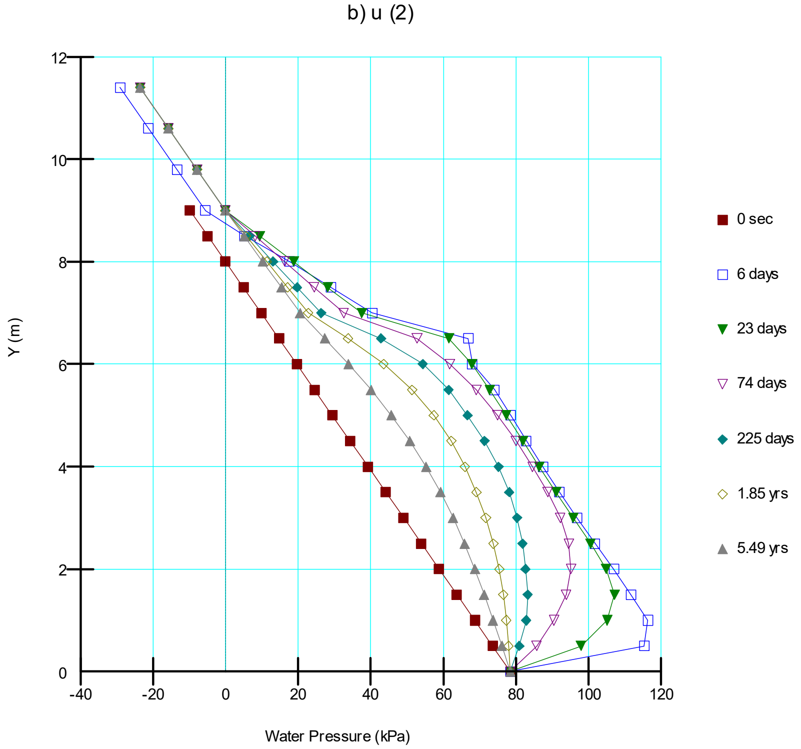

Figure 16. Long-term dissipation of excess pore-water pressures.

Figure 17 shows the long-term consolidation settlement profiles under the embankment. The maximum computed settlement after 5.5 years is around 0.87 m (870 mm), which is close to the actual measured maximum settlement of around 0.8 m. Once again, attempts could be made to alter the material properties to try to obtain a closer match. However, that is beyond the objective of this illustrative example.

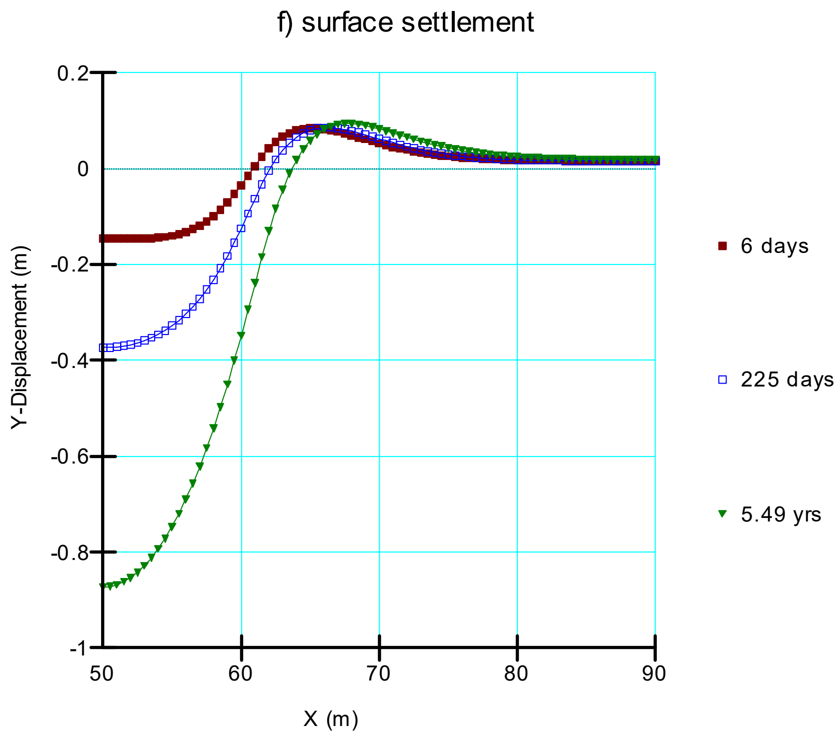

Figure 17. Long-term settlement of the original ground surface.

The computed horizontal movements at the toe of Embankment B are presented in Figure 18. At the end of construction on Day 6, the maximum computed lateral movement is around 170 mm. During the long consolidation period, the computed results show the lateral movement increasing to 233 mm. The field inclinometer profiles are shown in Figure 19. At the end of construction, the lateral movement was only about 25 mm, but then slowly increased during the consolidation to about 130 mm. The agreement between measured and computed deflections after 5 years is reasonably good. The measured and computed lateral deflections at the end of the fill placement, however, are markedly different. The reason for this difference is not clear, as there does not appear to be any intuitive logical reason for this. Of greater significance than the magnitude of the lateral deflections is the position of the maximum displacement that occurs in the soft clay just below the desiccated crust. This is also the zone where the failure slip surface was in Embankment A

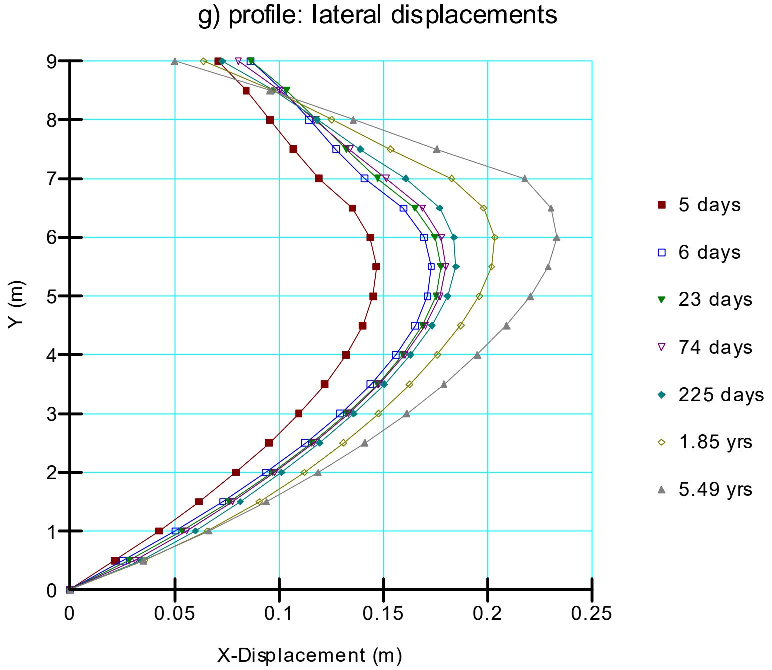

Figure 18. Computed lateral deflections at the toe of the embankment.

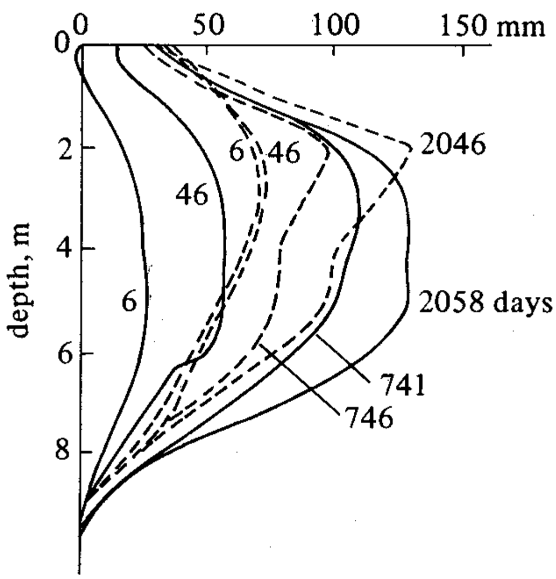

Figure 19. Field inclinometer profiles (solid lines) at the toe of Embankment B (Wood,1990 p. 406).

Summary and Conclusions

There is much more that could be done in analyzing the deformation response of these two embankments. A great amount of field and laboratory measurements are available. This data could be used to refine the analysis and more closely simulate the observed behavior. For example, the clay could be divided into various layers with each layer having slightly different properties. The soft clay immediately under the desiccated crust has a much higher organic content than the underlying soils. The higher organic content is normally associated with an increase in compressibility and hydraulic conductivity. In fact, the slope of the isotropic compression line (Lambda) was measured to be around 0.7 and 1.0 between depths of 2 and 4 m. Incidentally, this depth range corresponds to the location of the uniform lateral displacements and large settlements.

Of significance is that reasonable agreement between the measured and computed values for key deformation behaviors (that is, settlement, pore-water pressure, and lateral deformations) can be obtained with a simple set of material properties and boundary conditions. Furthermore, and perhaps more importantly, the occurrence of failure at the end of construction was appropriately predicted for Embankment A.

Obtaining reasonable results from a simplified approach of a real field case shows that it is not always necessary to try and duplicate all of the field intricacies. Useful and meaningful results can be obtained from a simplified numerical model of the actual field conditions. Whether this is true in all cases must be judged in light of the objective of the analysis.

References

Leroueil, S., Magnan, J.P., and Tavenas, F. 1990. Embankments on Soft Clay. Ellis Horwood, New York.

Wood, D.M. 1990. Soil Behaviour and Critical State Soil Mechanics. Cambridge University Press, Cambridge.